arXiv:1506.08020v2 [cond-mat.quant-gas] 22 Apr 2016

Spectroscopic Signatures for Bose-Einstein Condensation of Dark Excitons in a Trap

Mussie Beian[1,2], Mathieu Alloing[2], Romain Anankine[2], Edmond Cambril[3], Kamel Merghem[3], Carmen Gomez Carbonell[3], Aristide Lemaître[3] and François Dubin[1,2]
[1] *ICFO-The Institute of Photonic Sciences, Av. Carl Friedrich Gauss, num. 3, 08860 Castelldefels, Spain*
[2] *UPMC Univ Paris 06, CNRS-UMR 7588, Institut des NanoSciences de Paris, 4 Place Jussieu, F-75005 Paris, France and*
[3] *Laboratoire de Photonique et Nanostructures, LPN/CNRS, Route de Nozay, 91460 Marcoussis, France*

(Dated: April 25, 2016)

We study spatially indirect excitons confined in a 10 μm wide electrostatic trap. At sub-Kelvin bath temperatures, we show that the optical emission from the trap is anomalously weak in a regime where the excitons photoluminescence is homogeneously broadened and narrow-band. Particularly, we observe a loss of photoluminescence below a few Kelvin which violates classical expectations. Through a careful calibration of our experiments, we show that the photoluminescence loss can only be interpreted as the signature for Bose-Einstein stimulation of excitons from bright to dark states.

PACS numbers: 03.75.Hh,73.63.Hs,78.47.jd

I. INTRODUCTION

Bose-Einstein condensation constitutes a striking quantum phase transition in which, in the simplest approximation, a macroscopic ensemble of quantum particles ends in the lowest energy state, below some critical temperature [1]. Bose-Einstein condensation (BEC) was demonstrated for atomic gases, thanks to a thorough control over the cooling of laser-trapped atomic vapours. Low enough temperatures ($\sim \mu$K) were reached at the cost of complex evaporation techniques, and pure Bose-Einstein condensates were demonstrated. For that, elegant time-of flight absorption imaging was used to directly infer the momentum distribution before atoms are released from the trap.

For semiconductor excitons, boson-like particles which were considered already long ago to demonstrate Bose-Einstein condensation [2–4], experimental and theoretical research have mostly considered bright excitons due to their photoluminescence emission [5]. For such optically active excitons, BEC has to lead to a macroscopic population in the $\mathbf{k}$=0 motional state, which is the most efficiently coupled to light. A strong and narrow-band photoluminescence has then been searched as the signature for BEC. This has lead to very large progress in the understanding of exciton gases at low temperatures, but not to unambiguous signatures for Bose-Einstein condensation to the best of our knowledge.

Recently, M. Combescot and co-workers [6] brought forward a simple reason that could well explain the lack of consensus regarding Bose-Einstein condensation of excitons. For widely studied GaAs materials, the authors argumentation relies on the underlying fermionic nature of excitons, which are made of Coulomb bound electrons and holes, with "spins" equal to ($\pm 1/2$) and ($\pm 3/2$) respectively. Hence, excitons can carry a total spin (± 2). They are then optically dark and do not experience repulsive interband Coulomb scatterings, unlike optically bright excitons which carry a total spin (± 1) and then couple to light fields. The energy splitting between bright and dark states leads to an extensive energy difference between bright and dark exciton condensates, such that BEC inevitably yields a macroscopic population of dark excitons [6, 7]. For excitons in GaAs double quantum wells this splitting is in the range of a few micro-eV [8]. Accordingly, the extensive energy difference between bright and dark condensates is of the order of a milli-eV for 10^3 condensed excitons.

The conclusions reached by Combescot et al. [6] are in striking contrast with the long search for a condensate of optically active excitons [5]. Although it is analogous to spinor atomic gases or superfluid helium [10, 11], the dark state condensation leads to an anomalous darkening of the photoluminescence emission as the excitons temperature is decreased. By contrast, it is classically expected that the exciton photoluminescence is enhanced as the excitons temperature is lowered [12, 13]. In recent years, experimental works have reported observations that support the key role played by dark states for the low-temperature physics of exciton gases. These observations were made with spatially indirect or dipolar excitons[14–18], injected optically in a quantum well heterostructure. A surprisingly dark photoluminescence has thus been revealed [14, 18], and more importantly it was found that a microscopic and dark drop of excitons exhibited a long-range spatial coherence at sub-Kelvin bath temperatures [18]. The latter behaviour signalled clearly a quantum statistical regime. However, experiments suffer from a lack of control, e.g. from a large inhomogeneous broadening [14] or from the inability to control the exciton density [18].

Here, we report robust signatures for excitons condensation in optically dark states at sub-Kelvin bath temperatures. Evidences are obtained by confining long-lived indirect excitons (of a GaAs double quantum well) in a 10 μm wide dipole trap. Long after optical loading of the trap, in a regime where we expect to have a dilute gas at thermal equilibrium, we show that our experiments reach unprecedented performances: First, the exciton trap allows a quantitative variation of the excitons temperature at a fixed density. Also, the photoluminescence emitted is homogeneously broadened and narrow-band (300

μeV wide) when $\approx 10^4$ excitons are trapped at T_b=330 mK. In these well controlled conditions, we show that the photoluminescence darkens anomalously below a critical temperature $\sim$ 2K. After carefully excluding the effect of incoherent losses, we show that the photoluminescence darkening can only be interpreted by the quantum condensation of trapped excitons in the lowest energy dark states. At sub-Kelvin temperatures we estimate that 80% of excitons are quantum condensed in these dark states.

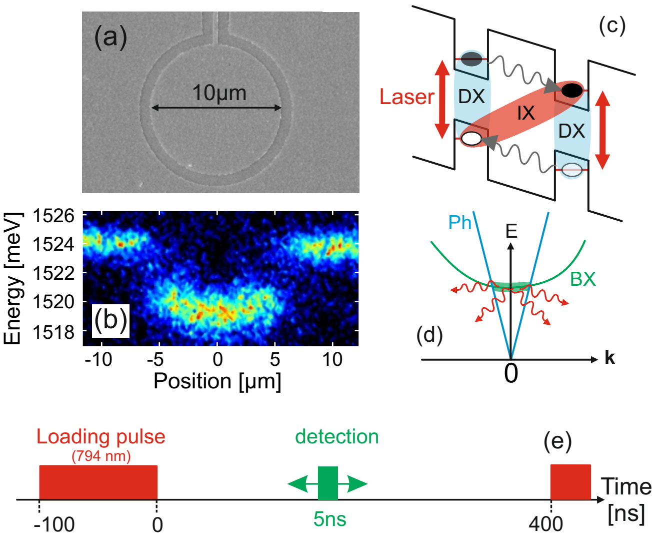

FIG. 1: (a) Electron microscope image of the surface electrodes constituting the electrostatic trap. (b) Spatial profile of the confining potential realized when the center electrode is biased at (-4.8V) while the outer electrode is biased at (-3.5V) at T_b=330 mK. The confinement profile is measured by injecting a very dilute and linearly shaped cloud of indirect excitons along the horizontal axis of the trap. (c) Sketch of the optical injection of indirect excitons (IX), through the resonant excitation of direct excitons (DX). IXs are finally created once electronic carriers have thermalized towards minimum energy states (wavy grey lines). (d) The reemitted photoluminescence (wavy red arrows) is only due to the radiative recombination of lowest energy ($\mathbf{k}\sim 0$) bright excitons (BX), i.e. lying at an energy smaller than the intersection between excitonic (BX) and photonic (Ph) bands. (e) Our experiments rely on a 100 ns long loading pulse while the exciton dynamics is monitored in a 5 ns long and running time window which follows each laser pulse. This sequence is repeated at 2 MHz.

II. EXPERIMENTAL METHODS

As illustrated in Figure 1, we probe spatially indirect excitons in a GaAs/AlGaAs double quantum well (DQW). Indirect excitons form in such heterostructures by applying an electric field perpendicular to the quantum wells. In our experiments, this is achieved by biasing two independent and semi-transparent metallic electrodes deposited on the surface of a field-effect device embedding the DQW (Fig. 1.a, see also [21] for details). This ensures that minimum energy levels for electrons and holes lie in distinct quantum wells (Fig. 1.c). In the following experiments, negative biases are applied to the two electrodes, with a larger one onto the central (trap) electrode compared to the outer (guard) electrode. As a result, we create a $\sim$10 μm wide trap of $\sim$5 meV depth (Fig. 1.b), indirect excitons being attracted towards the regions where the electric field is the strongest [15, 20].

Figure 1.c-e shows how excitons are injected in our studies: we use a 100 ns long laser excitation (at 2 MHz repetition rate) tuned on resonance with the direct exciton absorption of the DQW. Thus, the fraction of excess carriers photo-injected in the trap is efficiently damped, as confirmed by the low photo-current emission ($\sim$ 10-100 pA while the dark current is less than 10 pA). Also, the laser beam is set with a 8 μm waist such that it covers the entire trap where it yields a spatially homogeneous gas of indirect excitons after electrons and holes have tunnelled towards their respective minimum energy states.

Once the electrostatic trap has been optically loaded, we quantify the relative occupation of the excitons "spin" states as the total density is decreased by radiative recombination of bright indirect excitons (Fig. 1.d). This is achieved by varying the delay to the laser excitation (Fig. 1.e) while monitoring the integrated intensity of the photoluminescence, its spectral linewidth and energy position. The latter quantity, E_X, is used to quantify the total density, i.e., including both bright and dark excitons. Indeed, E_X reflects repulsive dipolar interactions between indirect excitons [22–24]. At first order, this contribution yields a blue-shift of the photoluminescence energy which scales as $u_0 n_x$, n_x denoting the exciton density. The exact magnitude of u_0 is still investigated theoretically, however it seems accepted that $u_0 n_x \sim$ 1meV for $n_x \sim 10^{10}$ cm^{-2} [22]. In our experiments the blue shift of the photoluminescence emission is inferred by comparing E_X to its value at the latest delays ($\sim$ 300 ns after termination of the laser excitation). Moreover, the photoluminescence integrated intensity (I_X) allows us to extract the fraction of bright excitons in the trap. Indeed, I_X is directly given by the product between the density of bright excitons and their optical decay rate ($1/\tau_{\text{opt}}$). By comparing the variations of I_X and E_X, we then infer the fraction of dark excitons. Finally, to estimate the strength of inhomogeneous broadening but also to confirm that indirect excitons are brought to lower temperatures as T_b is decreased, we analyze the photoluminescence linewidth (Γ_X) together with the spatial distribution of the exciton cloud in the trap.

III. SPECTROSCOPY OF INDIRECT EXCITONS TRAPPED AT T_b= 330 MK

Figure 2 quantifies the time evolution of I_X, Γ_X and E_X at the lowest bath temperature (T_b= 330 mK). Fig. 2.a shows that the photoluminescence integrated intensity and its emisson energy follow exponential-like decays (within the precision of our measurements), with characteristic times of about 60 and 120 ns respectively. This difference proves that the overall exciton density decays slower than its sole bright component. Also, in Figure 2.a we note that $\mathrm{E_X}$ decreases by $\sim$ 5 meV across the delay range that we explore. This suggests that the trap is full at the end of the laser excitation. The exciton density decreases from $\sim$5 10^{10} cm^{-2} at the termination of the laser pulse, to $\sim 10^9$ cm^{-2} at very long delays, that is at τ $\sim$250 ns when $\mathrm{E_X}$ becomes essentially constant.

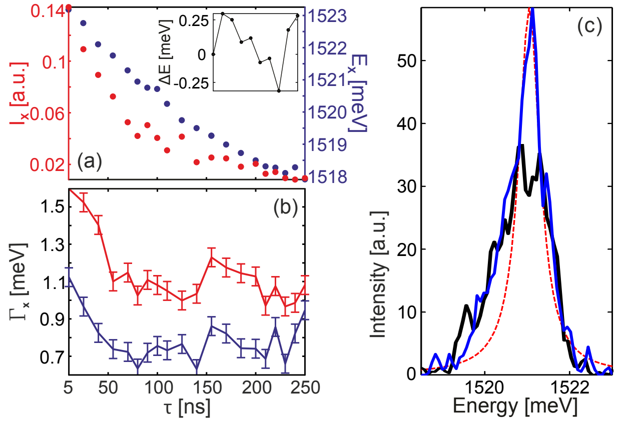

FIG. 2: (a) Integrated intensity ($\mathrm{I_X}$, red points) and energy ($\mathrm{E_X}$, blue points) of the photoluminescence as a function of the delay to the termination of the laser excitation (τ). The inset shows the variation of $\mathrm{E_X}$ between 10 successive one-minute acquisitions. (b) Dynamics of the photoluminescence spectral width (Γ_X) computed by accumulating directly 10 successive spectra (red) or by evaluating a statistical average (blue). (c) Photoluminesence spectra measured in two distinct one-minute interval (blue and black). The dashed red line shows a Lorentzian fit with 300 μeV spectral width. Measurements are all taken at $\mathrm{T_b}$=330 mK, in a 3 μm wide region at the center of the trap and for a 1 μW mean laser excitation power.

Fig. 2.b shows the dynamics of the photoluminescence spectral width Γ_X at $\mathrm{T_b}$=330 mK. We first note that Γ_X rapidly decreases in the first $\sim$70 ns after the laser excitation, and then remains essentially constant. We interpret the initial decrease of Γ_X as a manifestation of the excitons thermalisation in the trap. Indeed, it takes a few tens of nanoseconds to evacuate the laser induced heating of the heterostructure [25]. Furthermore, we can not exclude that the transient photocurrent, concentrated during and shortly after the laser pulse, contributes to the initial broadening of the photoluminescence. By contrast, at longer delays, $\tau \gtrsim$ 70-100 ns, Γ_X is essentially constant in a regime where the exciton gas is dilute since $n_\mathrm{x} a_\mathrm{X}^2 \leq$0.3, a_X $\sim$20 nm being the exciton Bohr radius [27]. This behaviour is expected since exciton-exciton interactions do not yield a significant homogeneous broadening [23, 29] across this range of densities ($n_\mathrm{x} \lesssim$ 3 10^{10} cm^{-2}).

In the measurements shown in Figure 2, the photoluminescence signal is in general very weak (for Fig. 2.c the peak intensity is $\sim$ 50 photons/min for a 5 ns integration window repeated at 2 MHz). That is why our studies rely on extended acquisitions. At first, we computed the photoluminescence spectrum averaged over an ensemble of 10 successive one-minute acquisitions. As shown in Fig. 2.b, this leads to $\Gamma_\mathrm{X}$$\sim$ 1 meV sufficiently long after the loading laser pulse. We have also studied the photoluminescence spectrum by evaluating the statistical average over the same 10 realisations, as also shown in Fig. 2.b. Remarkably, the latter approach yields a spectral narrowing $\sim$ 0.5 meV, so that Γ_X can become as narrow as a few hundreds of μeV. The difference between the two processing techniques reflects the energy fluctuations of the electrostatic trapping potential. Indeed, the inset in Fig. 2.a shows that $\mathrm{E_X}$ varies by as much as 500 μeV over an ensemble of ten successive one-minute acquisitions.

Fig.2.c illustrates the impact of spectral diffusion. It compares two single-shot (one-minute) acquisitions recorded 150 ns after termination of the laser excitation, i.e. for an exciton density n_x $\sim$ 2 10^{10} cm^{-2}; one realisation shows a rather broad photoluminescence ($\sim$ 1.5 meV) while the second spectrum uncovers a fine structure with a 300 μeV wide lorentzian line superposed onto spectrally wider component. The latter experimental run allows concluding that we observe an homogeneously broadened gas of indirect excitons. Unfortunately, spectral diffusion blurs the photoluminescence spectrum. It introduces random flucuations of the electrostatic confinement during the measurement time, which lasts over half a day for basic acquisition at a single bath temperature. In this time interval, we note strong spectral fluctuations, as the ones shown in Figure 2, at a rate limited by the low photoluminescence emission from the trap ($\sim$ 10 sec). However, these fluctuations only induce 10-20% variations of the integrated intensity. This indicates that our device allows estimating the density of bright excitons in the trap by monitoring $\mathrm{I_X}$. On the other hand, to estimate the total density of excitons through $\mathrm{E_X}$, our studies are limited by spectral diffusion to about 500 μeV, yielding a precision of the order of 5 10^9 cm^{-2} on the exciton density.

IV. EVIDENCE FOR EXCITON THERMALISATION TO SUB-KELVIN BATH TEMPERATURES

For indirect excitons confined in our trap, the critical temperature for Bose-Einstein condensation is estimated in the range of a few Kelvin for n_x $\sim$ 10^{10} cm^{-2} [9]. For the experiments shown in Figure 2, this range of densities is reached about 150-200 ns after the laser excitation, i.e., in the regime where the photoluminescence emitted by bright excitons is homogeneously broadened and spectrally narrow-band. In such conditions, one naturally wonders if the trapped gas behaves classically, or, on the contrary, does it behave quantum statistically since these experiments are performed at $\mathrm{T_b}$=0.33 K.

As mentioned previously, to tackle this issue we followed Combescot and co-workers [30] and quantified the occupation of bright and dark exciton states as the bath temperature is lowered. We restricted our studies to a parameter space where experimental conditions are constant, that is the photo-current generated by the laser excitation, the depth and the spatial profile of the trapping potential. This sets well defined experimental conditions. Also, it sets the range of accessible bath temperatures to $0.33 \leq T_b \leq 3.5$ Kelvins.

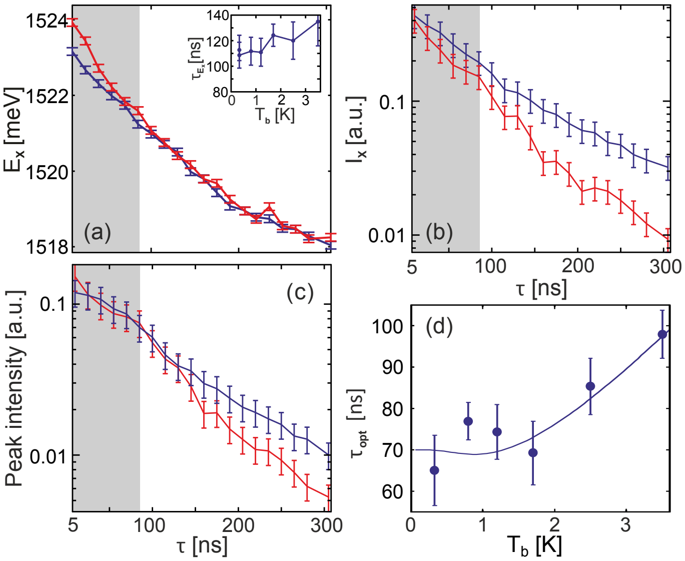

FIG. 3: (a) Energy of the photoluminescence (E_X) at T_b=330 mK (red) and 2.5K (blue). (b) Decay of the photoluminescence integrated intensity (I_X). (c) Dynamics of the maximum of the photoluminescence spectrum. (d) Optical decay time τ_{opt} of the photoluminescence integrated intensity, versus T_b. Experiments correspond to 3 days of continuous data acquisition, and the presented data have all been analyzed in a 3 μm wide region at the center of the trap.

Figure 3.a displays the energy of the photoluminescence as a function of time and for T_b= 0.33 and 2.5 K. It shows that E_X exhibits a very stable dynamics across this range of bath temperatures. We only note a slight deviation at short delays to the termination of the laser excitation ($\tau \leq$70 ns in the grey region in Figure 3). We attribute this deviation to a varying transient photocurrent. This inevitable photocurrent alters the internal electric field and then E_X too. The latter can no longer be simply used to extract the overall exciton density. On the other hand, E_X is mostly unchanged beyond the transient regime ($\tau \geq$80 ns) when we increase T_b up to 3.5 K. At long delays ($\tau \sim$ 300 ns) it varies by less than 500 μeV reflecting the fluctuations of the trap depth (∼8%), dipolar repulsions between excitons yielding a vanishing correction to E_X in this very dilute regime. At higher densities, i.e. for $80 \lesssim \tau \lesssim 250$ ns which corresponds to $5\ 10^9 \lesssim n_x \lesssim 3\ 10^{10}$ cm^{-2}, we observe again that E_X varies by less than 500 μeV between 0.33 and 2.5 K. Given the stability of the trapping potential, we are lead to conclude that exciton-exciton interactions exhibit a negligible temperature dependence in our experiments. This observation contrasts with recent works reporting an increase of excitonic correlations for bath temperatures below 2.5 Kelvins [14]. It was then concluded that a dark liquid of indirect excitons was building up. Instead, our experiments reveal that thermal activation, by increasing the bath temperature up to 3.5 K, varies exciton-exciton interactions by less than our instrumental precision (∼ 500 μeV). This supports our estimation of the exciton density which places our studies well in the dilute regime. Trapped excitons behaving as a weakly interacting gaseous ensemble, quantum statistical correlations can be understood in the framework of Bose-Einstein condensation.

Interestingly, at $T_b \leq$ 3.5K and for $\tau \geq$80 ns we noted that the dynamics of E_X can be approximately modelled by a mono-exponential decay. The inset in Figure 3.a shows the extracted time constants. For each bath temperature the precision of the fitting routine is about 20 ns, sufficient to note that the decay time varies weakly with the bath temperature. It is bound to about 100 ns which further supports that the total density of excitons has a stable dynamics across this range of bath temperatures.

Unlike the total exciton density, the occupation of bright states strongly depends on the bath temperature. This behaviour is shown in Figure 3.b that presents the dynamics of the photoluminescence integrated intensity I_X at T_b=0.33 and 2.5 K. The transient regime (grey region) constitutes the only region where I_X varies weakly with T_b. It confirms that bright excitons are not completely thermalised, otherwise the population in the lowest energy bright states would increase between 2.5 and 0.33 K, and so I_X would increase. Beyond the transient regime, Fig. 3.b clearly shows that the photoluminescence intensity drops faster as the bath temperature is lowered. In an attempt to quantify this decrease, we modelled the decay of I_X with a simple exponential after the transient regime, i.e., for $\tau \geq$80 ns. The resulting decay times τ_{opt} are displayed in Fig.3.d, as a function of T_b. It shows that the precision of the fitting routine is reasonable, being of the order of 10 ns. Thus, we observe that τ_{opt} drops from ∼ 100 ns at T_b=3.5 K to ∼ 70 ns at 1.5 K, τ_{opt} being rather constant at lower temperatures within the precision of our analysis.

The optical decay time τ_{opt} is expected to vary with the exciton temperature [13, 31]. Indeed, only coldest bright excitons, with a kinetic energy lower than about 150 μeV (∼ 1.5K), contribute to the photoluminescence. As a result, bright excitons decay faster as one lowers their temperature, simply because they can "spend" more time in the radiative region of the energy band (Fig.1.c). In a classical regime, i.e., when excitonic states are thermally populated, it was shown that τ_{opt} decreases linearly with the exciton temperature [26], provided that this temperature is sufficiently large compared to 1.5K. Otherwise, classical approximations no longer hold since the exciton

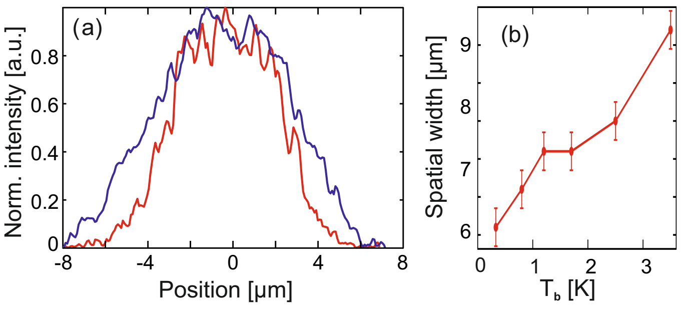

FIG. 4: (a) Spatial profile of I_X across the trap, at T_b=330 mK (red) and 3.5K (blue). (b) Spatial width of the exciton cloud as a function of T_b, measured as the full-width-at-half maximum. Measurements are all evaluated at τ=190 ns.

gas becomes statistically degenerate. In this latter case, the optical decay time of the photoluminescence saturates for an exciton temperature of about 1.5 K when $n_X \sim 10^{10}$ cm^{-2}, yielding a photoluminescence decay rate equal to twice the intrinsic radiative lifetime [13, 31]. Remarkably, Figure 3.d reproduces this behaviour: indeed our findings are well reproduced using the theoretical model detailed in Ref [31]. This leads us to two main conclusions: (i) trapped excitons are thermalised to lower temperatures as T_b is decreased, the thermalisation possibly occurring to the bath temperature (ii) the saturation of τ_{opt} is consistent with a statistically degenerate gas of indirect excitons.

The cooling of trapped excitons by lowering T_b is supported further by the spatial profile of the photoluminescence. Figure 4 shows that it contracts by over 30 % between 3.5 and 0.33 K. Thus, at T_b=330 mK, the cloud is concentrated at the center of the trap where bright excitons emit a top-hat like photoluminescence, as expected for a cold gas. Finally, let us note that the saturation of τ_{opt} to $\sim$ 65 ns in our experiments leads to a radiative lifetime of about 30 ns for our heterostructure. This estimation is compatible with numerical simulations for DQW heterostructures [27], given that we estimate the internal electric-field to about 20-40 kV.cm^{-1}, the precision being here limited by the screening of the internal field by photo-injected and trapped carriers [28].

V. ANOMALOUS PHOTOLUMINESCENCE DARKENING AND DARK-STATE QUANTUM CONDENSATION

The results displayed in Figures 3 and 4 demonstrate unambiguously that trapped excitons are brought to lower temperatures while T_b is decreased. Among the signatures for such cooling, we have shown that the optical decay time of the photoluminescence τ_{opt} decreases by almost a factor 2 when the bath temperature is reduced from 3.5 to 0.33 Kelvins. Accordingly, the intensity of the photoluminescence is expected to increase, because our experiments are performed at a fixed overall exciton density n_X while the photoluminescence emission scales as n_X/τ_{opt}. However, we observe just the opposite behaviour. For $\tau \sim$ 150 ns, Fig. 3.b shows that the photoluminescence integrated intensity is 3 times smaller at T_b=330 mK than at 2.5 K. Furthermore, Fig. 3.c signals that not only the integrated intensity is damped while the exciton gas is cooled, but also the peak intensity, which is even more surprising since the photoluminescence spectral width decreases by over 50% in this range of bath temperatures. This leads us to conclude that our experiments reveal a strong depletion of lowest energy bright excitons, which results in an anomalous darkening as the bath temperature is lowered to the sub-Kelvin regime. This conclusion is inevitable for our studies where the total density of excitons is conserved.

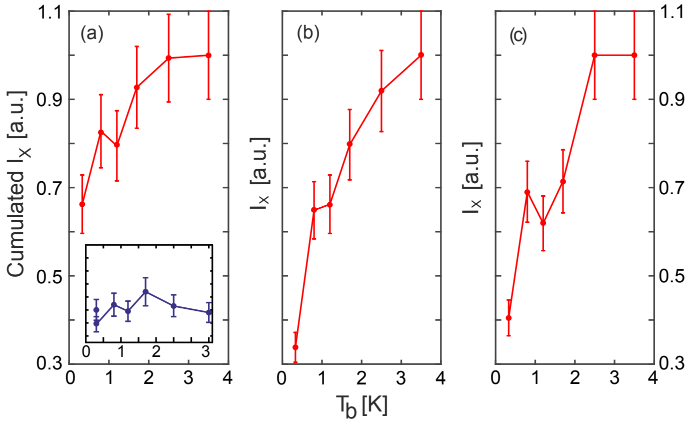

FIG. 5: (a) Cumulated integrated intensity measured from τ=80 ns, as a function of T_b. (b) Integrated intensity measured at τ=190 ns, i.e., for $n_x \sim 2\ 10^{10}$ cm^{-2}. The inset in the panel (a) shows the same measurement realised 5 ns after termination of the laser pulse. (c) Integrated intensity measured at τ=260 ns, i.e., for $n_x \sim 5\ 10^{9}$ cm^{-2}.

To interpret the photoluminescence darkening below a few Kelvin, we estimate first the maximum error of our measurements. For that, we analyse the photoluminescence cumulated integrated intensity, measured from τ=80 ns, that is after the transient regime discussed previously. The cumulated integrated intensity computes the total number of photons detected in our experiments for $\tau \geq$80 ns. It gives the total number of bright excitons that we have created and confined in the trap after the transient regime. Figure 5.a shows that the cumulated integrated intensity decreases by about 30% between 3.5 and 0.33 Kelvins. Accordingly, incoherent non-radiative losses can account for up to 30% of the photoluminescence darkening. These incoherent losses embrace the processes which can vary the rate of excitons radiative recombination in a temperature dependent manner, but also the processes that can lead to an escape of excitons from the trap. Resulting in a $\sim$30 % variations, altogether these processes are not sufficient to interpret our experiments. Indeed, Figure 5.b. shows that the amplitude of the photoluminescence darkening reaches approximately 70% 190 ns after the termination of the laser excitation and about 60% 60 ns later (τ=250 ns). We have shown that in this regime the photoluminescence is homogeneously broadened; we then have no other choice than to conclude that bright excitons are converted into dark excitons to possibly conserve the total density while excitons are cooled down to sub-Kelvin temperatures. This conclusion inevitably leads us to conclude that the darkening arises in a Bose condensed regime since the energy splitting between bright and dark states is only of a few μeV in DQWs, that is about 10-fold less than the thermal activation energy at our lowest bath temperature. Let us then assume that excitons are thermally distributed at T_b=3.5K, a reasonable hypothesis since the excitons degeneracy temperature is expected at about 2K. In this case, bright and dark excitonic states are equally populated at T_b=3.5K when thermal broadening is expected dominant. Starting from this distribution, we deduce that at T_b=330 mK the fraction of excitons in the dark states reaches $\sim$80 % 190 ns after the loading pulse, i.e., when the total exciton density is about 2 10^{10} cm^{-2}. Such an occupation of dark states then is highly non-classical. It quantitatively confirms, under well controlled conditions, the predicted Bose-Einstein condensation of dark excitons [6, 7].

VI. CONCLUSIONS

We would like to point out that our experiments, relying on time and spatially resolved spectroscopy, can only evidence the dark-state condensation through a loss of photoluminescence at exciton densities $n_X \sim 10^{10}$ cm^{-2}. To unambiguously relate this loss to quantum condensation into dark states, we have verified that non-radiative channels, others than stimulated scattering from low energy bright to dark excitons, can not account for our observations. Additionally, we have confirmed that a balance sheet between bright and dark occupations is made in a regime where the photoluminescence is homogeneously broadened at sub-Kelvin bath temperatures. As shown in Figure 4, we observe the anomalous photoluminescence darkening over a wide range of densities in the trap (0.5 10^{10} cm$^{-2}\lesssim n_x \lesssim 2\ 10^{10}$ cm^{-2}, corresponding to time delays after the loading laser pulse $150\lesssim \tau \lesssim 250$ ns), whereas at higher densities the darkening is not clearly marked. At lower densities our instrumental precision does not allow us to reach quantitative conclusions.

According to theoretical predictions [32], and also to recent experiments that we performed onto similar heterostructure [18], in the regime where we conclude that we have observed dark-state quantum condensation of indirect excitons, the exciton condensate is not only made of dark excitons. Instead, it consists of a dominant dark component coherently coupled to a weaker bright component. As a result, the exciton condensate can be viewed as "gray" and characterised by a weak coherent photoluminescence. The narrow-band emission that we observe at 330 mK is not incompatible with this conclusion, however a quantitative proof will require time and spatially resolved interferometry. This analysis lies beyond the scope of the present study.

Acknowledgements: The authors are grateful to Suzanne Dang for assistance and to Monique Combescot and Roland Combescot for a critical reading of the manuscript and for enlightening discussions. This work has been supported by the EU-ITN INDEX and EU-CIG X-BEC.

[1] *"Bose-Einstein Condensation"*, L.P. Pitaevskii, S. Stringari (Oxford university Press, 2003)
[2] S.A. Moskalenko, Fiz. Tverd. Tela (Leningrad) **4**, 276 (1962)
[3] J. M. Blatt et al., Phys. Rev. **126**, 1691 (1962)
[4] L.V. Keldysh and A.N. Kozlov, Sov. Phys. JETP **27**, 521 (1968)
[5] R. Zimmerman *"Bose-Einstein condensation fo excitons: promise and disapointment"* (Oxford. Univ. Press., Eds. A. L. Ivanov and S. G. Tikhodeev, 2008)
[6] M. Combescot, O. Betbeder-Matibet, R. Combescot, Phys. Rev. Lett. **99**, 176403 (2007)
[7] M. Combescot, M.N. Leuenberger, Solid State Comm. **149**, 567 (2009)
[8] E. Blackwood et al., Phys. Rev. B **50**, 14246 (1994)
[9] O. L. Berman, Y. E. Lozovik, D. W. Snoke, and R. D.. Coalson Phys. Rev. B **70**, 235310 (2004)
[10] A.J. Leggett *Quantum Liquids* (Oxford. Univ. Press, 2006)
[11] D.M. Stamper-Kurn, M. Ueda, Rev. Mod. Phys. **85**, 1191 (2013)
[12] B. Deveaud et al., Phys. Rev. Lett. **67**, 2355 (1991)
[13] A. Ivanov et al., Phys. Rev. B **59**, 5032 (1999)
[14] Y. Shilo et al., Nat. Comm. **4**, 2235 (2013)
[15] G. Schinner et al., Phys. Rev. Lett. **110**, 127403 (2013).
[16] A.V. Gorbunov, V.P. Timofeev, Sol. Stat. Comm. **157**, 6 (2013)
[17] A.A. High et al., Nature **483**, 584 (2012)
[18] M. Alloing et al., Europhys. Lett. **107**, 10012 (2014)
[19] D. Nandi, A.D.K. Finck, J.P. Eisenstein, L.N. Pfeiffer and K.W. West, Nature **488**, 481 (2012)
[20] A.A. High et al., Phys. Rev. Lett. **103**, 087403 (2009)
[21] M. Beian et al., Europhys. Lett. **110**, 27001 (2015)
[22] A. L. Ivanov, E. A. Muljarov, L. Mouchliadis, and R. Zimmermann, Phys. Rev. Lett. **104**, 179701 (2010)
[23] C. Schindler and R. Zimmermann, Phys. Rev. B **78**, 045313 (2008)
[24] B. Laikhtman. and R. Rapaport, Phys. Rev. B **80**, 195313 (2009)
[25] A. L. Ivanov, J. Phys.: Condens. Matter **16**, S3629 (2004)
[26] L.C. Andreani, F. Bassani, Phys. Rev. B **41**, 7536 (1990)
[27] K. Sivalertporn, L. Mouchliadis, A. L. Ivanov, R. Philp,

and E. A. Muljarov Phys. Rev. B **85**, 045207 (2012)
[28] M. Alloing et al., Sci. Rep. **3**, 1578 (2013)
[29] Z. Voros, D. W. Snoke, L. Pfeiffer, and K. West Phys. Rev. Lett. **103**, 016403 (2009)
[30] M. Combescot, R. Combescot, M. Alloing, F. Dubin, Europhys. Lett. **105**, 47011 (2014)
[31] A.I. Ivanov, P.B. Littlewood, H. Haug, J. of Lum. **87**, 189 (2000)
[32] R. Combescot and M. Combescot Phys. Rev. Lett. **109**, 026401 (2012)